Four-wave-mixing theory for two-photon generation of excitons in Cu_2O

I. V. Beloussov,[1,*] J. B. Ketterson,[2,†] and Y. Sun[2]
[1]*Institute of Applied Physics, Academy of Sciences of Moldova, 5 Academy Street, Kishinev MD-2028, Republic of Moldova*
[2]*Department of Physics and Astronomy, Northwestern University, Evanston, Illinois 60208, USA*
(Received 11 July 2009; published 23 December 2009)

We propose and examine theoretically a four-wave-mixing experiment in which excitons in Cu_2O are pumped directly into a state with wave vector $\mathbf{k}=\mathbf{0}$ by two counter-propagating cross-polarized laser pulses and which is subsequently probed by a third time-delayed pulse. Approximate analytical solutions of the time evolution equations are found which describe the time dependence of the exciton and photon densities. Most importantly, we obtain the dependence of the resulting phase-conjugated signal versus the delay time t_d between the probe and pump pulses. It is shown that the total number of photons generated in the course of the experiment is proportional to the areas of all three incoming pulses. The dependence of the resulting time-integrated signal on the delay time t_d is the same as the exciton density dependence on the time t. Hence, one may directly study the time evolution of the exciton condensate. The approximate analytical results are compared with a numerical solution of the evolution equations for a wide range of incident pulse intensities. It is noted that an exciton condensate arising by an alternate route can also be probed through a phase-conjugated two-photon process.

DOI: 10.1103/PhysRevB.80.245213 PACS number(s): 71.35.−y, 42.50.Md, 42.65.Sf

I. INTRODUCTION

Cuprous oxide has long been considered as a possible candidate for Bose-Einstein condensation (BEC) of excitons.[1–4] For the same density, the relatively small exciton mass would allow condensation at temperatures much higher than those associated atomic systems such as liquid helium or a gas of trapped alkali-metal atoms.[5] Since the first experiment showing Bose-Einstein statistics of orthoexcitons in Cu_2O,[6] attempts have been made to observe BEC in this nearly ideal Bose gas system.[7–9] Bose-Einstein condensation of paraexcitons was reported by Lin and Wolfe[10] but the interpretation remains uncertain. However BEC of the orthoexcitonic system has not been reported, possibly due to ortho-para conversion restricting the achievable densities. Recently Jang and Wolfe[11] proposed another decay channel: the formation of biexcitons followed by recombination.

Previous investigations[6–9] have primarily involved one-photon absorption. Electron-hole pairs generated by this process relax toward the 1*s* state of the lowest excitonic series. The 1*s* level is split by the electron-hole exchange interaction into triply degenerate Γ_{25}^{+} orthoexciton states and a Γ_{2}^{+} singlet paraexciton state. One decay mode of the 1*s* orthoexcitons involves the creation of a parity-conserving Γ_{12}^{-} optical phonon. The line shape of the associated luminescence spectrum then provides a direct way to measure the velocity distribution of the nearly free-exciton gas.[6,8–10] The relaxation of optically generated electron-hole pairs results in a temperature rise of the exciton gas (up to about 100 K) and the density of the orthoexcitons always saturates below the critical density for BEC.[7] Hence, BEC of the orthoexcitons has not been realized by the one-photon excitation.

Recently, several studies on resonant two-photon excitation of 1*s* excitons at low temperatures have been reported.[12–17] The interest was driven by the possibility that a cooler high-density exciton gas can be produced by resonant excitation. Direct electron-hole recombination emission and phonon-assisted electric dipole radiative transitions involving Γ_{12}^{-} longitudinal optical phonons were observed. A strongly enhanced direct electron-hole recombination emission has been interpreted as resonant second-harmonic generation.[12] Further high-resolution two-photon spectroscopic studies of orthoexcitons near 2 K (Ref. 16) revealed a suppression of orthoexciton emission when the two-photon energy was within a narrow range centered on the resonance, which was interpreted as a quadrupole polariton effect.

Second harmonic generation and hyper-Raman scattering of the Γ_{12}^{-} phonon have been observed when the two-photon energy is resonant with the 1*s* orthoexciton.[12,15] The intensities of the second-harmonic and hyper-Raman-scattering signals do not depend sensitively on the quality of samples. Conversely, the luminescence intensity depends very sensitively on the sample quality[12] and strong orthoexciton luminescence was observed using a high-purity crystal.[13] It has been suggested that nearly zero-momentum orthoexcitons can be directly generated by two-photon absorption and the Bose-Einstein statistical properties of the orthoexciton system have been discussed.

In yet another study 1*s* orthoexciton luminescence spectra in Cu_2O resulting from two-photon resonant pumping to the 1*s* and 2*s* levels were studied over a wide temperature range (from 1.8 to 70 K).[17] The direct electron-hole recombination emission and phonon-assisted, electric dipole radiative transition were observed at all temperatures. The intensities of the peaks from these two states are found to have very different temperature dependences that also depend on whether the 1*s* or 2*s* level was resonantly excited. At low temperature, the intensity of the direct electron-hole recombination line was greatly enhanced when the 1*s* level was resonantly excited. As in the earlier studies, the emission was observed to strongly peak in the direction of the pump beam. Here it was proposed that the effect results from quadrupole orthoexciton-polariton waves, generated continuously along the beam path by two-photon absorption from the incoming

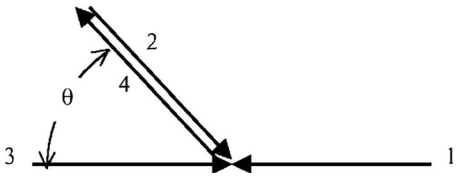

FIG. 1. Scheme of four-wave mixing.

pump beam, which convert into light at the exiting surface. This process would appear to be somewhat different from the resonant quadrupole second-harmonic generation that was proposed[12] to explain the resonant enhancement of direct electron-hole recombination emission. However it is related to one-photon experiments in which coherent quadrupole-exciton polaritons, on both branches, are resonantly generated at the entering surface and their subsequent interference is observed as an oscillatory time-dependent decay (so-called quantum beats).[18] It was also observed that under two-photon pumping the exiting beam had a divergence that was several times larger than that of the pump beam; the latter effect has been recently examined in much greater detail and the beam spreading was interpreted as arising from scattering of the exciton component of the polariton wave.[19] Further studies showed anomalous Fresnel coefficients for polaritons[20] and, at high pump intensities, suppressed molecule formation for polaritons.[21]

An interesting type of experiments on two-photon excitation involves pumping directly into a state $\mathbf{k}=\mathbf{0}$.[22] To perform such experiments, it is necessary to split the incident beam into two or more pulses and to direct them on the sample from different directions. Employing an optical delay line one can control the arrival time of any of the pulses on the sample. Consider the configuration shown schematically in Fig. 1.

The pump beams 1 and 3 with wave vectors $\mathbf{k}_1$ and $\mathbf{k}_3(\mathbf{k}_3=-\mathbf{k}_1)$, respectively, generate in the system a macroscopic coherent state of excitons with wave vector $\mathbf{k}=\mathbf{k}_1+\mathbf{k}_3=\mathbf{0}$ that we call a condensate. This is not an equilibrium state. If we now act on the system by the probe beam 2 with wave vector $\mathbf{k}_2(|\mathbf{k}_2|=|\mathbf{k}_1|)$, this results in a stimulated radiation of condensate excitons and a phase-conjugated beam 4 with wave vector $\mathbf{k}_4=-\mathbf{k}_2$ arises. We will show that the resulting beam 4 can be used to monitor the condensate decay after its generation. Note that a thermal distribution of orthoexcitons does not lead to the formation of macroscopic coherent back scattering. Similar methods, generally termed *four-wave mixing*, have proved to be powerful tools to investigate, in a direct manner, coherent excitations in various systems, along with the scattering processes which destroy this coherence.[23,24]

This paper is organized as follows. In Sec. II we discuss in detail the basic physical assumptions used in our investigation and formulate a theoretical model based on a simple Hamiltonian to describe the process of two-photon transitions from the ground state of the crystal to the orthoexciton state. Using these assumptions, we obtain from the Hamiltonian the basic equations for macroscopic amplitudes of coherent excitons and photons. In Sec. III we propose a specific experimental configuration for which the equations for the amplitudes have the simplest form. In Sec. IV we solve this set of equations using an external field approximation where we ignore a backward influence of generated excitons on the incident pulses. For the subsequent numerical results, we estimate in Sec. V the interaction constant that is contained in our model Hamiltonian. In Sec. VI we compare the results of numerical solutions of the equations describing time evolution of the system with the analytical results obtained in the external field approximation and discuss them. In Sec. VII we present our conclusions.

II. BASIC ASSUMPTIONS AND THE THEORETICAL MODEL

We now discuss the principal assumptions that allow a substantial theoretical simplification of the phenomena to be examined. (i) We will treat the excitons generated by the pump beams as a gas of ideal bosons. According to Ref. 1, this description is sufficient if the following inequalities are fulfilled:

$$n_{ex}a_{ex}^3 \ll 1/8\pi, \quad n_{ex}U \ll \hbar^2/2m_{ex}a_{ex}^2, \tag{1}$$

where n_{ex} is the exciton density, a_{ex} and m_{ex} are their radius and effective mass, respectively, and $U=4\pi a_{ex}\hbar^2/m_{ex}$ is the exciton-exciton interaction constant. Since the exciton radius is small ($a_{ex}=7$ Å) and the two-photon transition probability from the ground state into an exciton state is low, inequalities [Eq. (1)] are well satisfied, even for relatively high-flux densities S (~ 1 GW/cm^2) when $n_{ex}\sim 10^{17}$ cm^{-3}.

(ii) For $S \lesssim 100$ MW/cm^2, we have $Un_{ex} \ll g\sqrt{n_{ex}}$; i.e., two-photon generation of orthoexcitons, governed by the effective interaction constant g, is large compared with exciton-exciton scattering. Therefore, we shall not take the exciton-exciton interactions into account.

(iii) We shall use a purely classical description, where the time-dependent state of the system is described only by the macroscopic coherent amplitudes of the interacting excitons and photons. If the interaction between the excitons and the photons was linear, their initial coherence would be retained at all subsequent times.[25] In this case, a total factorization of all the correlation functions describing the state of the quantum system would occur at any time. As a result, to describe its dynamics, it will be sufficient to only investigate the temporal evolution of the coherent amplitudes. The process of two-photon generation of excitons examined here is caused by a nonlinear interaction. Strictly speaking, it can lead to the loss of the initial coherence of the excitons and photons owing to the generation of quantum fluctuations which react back on the system. In such a case it is not sufficient to use only coherent amplitudes to describe the system. However, as was shown in Ref. 26, the influence of the quantum fluctuations on the initial coherent state only becomes important over times when they can "accumulate;" we will assume that *noncoherent* photons generated in the system leave the crystal before this occurs. The "decay of coherence" of the excitons is taken into account by introducing a phenomenological decay constant.

(iv) Our aim here is to investigate the propagation of two counter-propagating pump pulses and a delayed probe pulse.

This process is accompanied by the generation of a phase-conjugated signal. Strictly speaking, to treat this problem one needs to consider solutions of the dynamical equations which are nonuniform, not only in time but also in space, and which satisfy specific conditions at the crystal boundaries. However we will restrict ourselves to the simpler problem involving only the time evolution of the system. It should be a good approximation to regard the total electromagnetic field in the crystal as a superposition of two spatially uniform fields. The first of them, which we will assume has a specific envelope in time, is generated by external sources. The second field arises from a polarization of the medium resulting from exciton creation in the crystal by the first field. The equation for photon amplitudes involves a current density $j_\lambda(\mathbf{k},t)$ arising from the excitons as well as a damping Γ_{ph} that accounts the photon escape from the crystal. Our description not only allows for the generation of the phase-conjugated beam but also takes into account the influence that the excitons and photons so generated have on the three primary electromagnetic fields with wave vectors $\mathbf{k}_1$, $\mathbf{k}_3$, and $\mathbf{k}_2$. Strictly speaking, the approach is valid only for laser pulses in which the spatial extent exceeds the crystal dimensions. The phenomenological constant Γ_{ex} in equation for excitons amplitude takes into account the exciton dephasing.

We now introduce a model Hamiltonian that will be used to describe the dynamics of the system. The spin-orbit coupling splits the $1s$ yellow excitons in Cu_2O into a threefold degenerate ${}^3\Gamma_{25}^+$ (orthoexciton) state, with wave functions transforming as xy, yz, zx, and a single ${}^1\Gamma_2^+$ (paraexciton) state.[27] According to the selection rules, the two-photon transitions from the ground state into orthoexciton states are allowed but are forbidden for the paraexciton state. The following Hamiltonian describes two-photon excitation process into the three orthoexciton states (xy, yz, and zx) and incorporates assumptions (i) and (ii) (Ref. 22):

$$H = H_{ex} + H_{ph} + H_{int}, \tag{2}$$

$$H_{ex} = \sum_{\mathbf{k}} \hbar\omega_{ex}(\mathbf{k}) \sum_{\alpha=xy,yz,zx} \hat{a}_\alpha^\dagger(\mathbf{k})\hat{a}_\alpha(\mathbf{k}),$$

$$H_{ph} = \sum_{\mathbf{k}} \hbar\omega_{ph}(\mathbf{k}) \sum_{\lambda=1,2} \hat{c}_\lambda^\dagger(\mathbf{k})\hat{c}_\lambda(\mathbf{k}), \tag{3}$$

$$H_{int} = \frac{1}{2!\sqrt{V}} \sum_{\mathbf{k}_1,\mathbf{k}_2} \sum_{\alpha=xy,yz,zx} \sum_{\lambda_1,\lambda_2=1,2} g_\alpha^{(\lambda_1,\lambda_2)}(\mathbf{k}_1,\mathbf{k}_2) \times [\hat{a}_\alpha^\dagger(\mathbf{k}_1+\mathbf{k}_2)\hat{c}_{\lambda_1}(\mathbf{k}_1)\hat{c}_{\lambda_2}(\mathbf{k}_2) + \text{H.c.}], \tag{4}$$

here $\hbar\omega_{ex}(\mathbf{k}) = \hbar\omega_{ex}(0) + \hbar^2\mathbf{k}^2/2m_{ex}$ and $\hbar\omega_{ph}(\mathbf{k}) = \hbar c|\mathbf{k}|/\sqrt{\varepsilon_b}$ are the energies of the excitons and photons in the states with wave vector $\mathbf{k}$, respectively, ε_b is background permittivity of the medium, and c is the speed of light in vacuum. The creation $\hat{a}_\alpha^\dagger(\mathbf{k})$, $\hat{c}_\lambda^\dagger(\mathbf{k})$ and destruction $\hat{a}_\alpha(\mathbf{k})$, $\hat{c}_\lambda(\mathbf{k})$ operators of α-excitons ($\alpha = xy, yz, zx$) and photons with polarization ($\lambda = 1, 2$) obey the Bose commutation relationships.

The interaction constants $g_\alpha^{(\lambda_1,\lambda_2)}(\mathbf{k}_1,\mathbf{k}_2)$ are proportional to matrix elements of the two-photon transitions calculated in second-order perturbation theory. Using the selection rules for these transitions,[27] we can write these constants in the form

$$g_{xy}^{(\lambda_1,\lambda_2)}(\mathbf{k}_1,\mathbf{k}_2) = e_x^{(\lambda_1)}(\mathbf{k}_1)e_y^{(\lambda_2)}(\mathbf{k}_2) + e_y^{(\lambda_1)}(\mathbf{k}_1)e_x^{(\lambda_2)}(\mathbf{k}_2),$$

$$g_{yz}^{(\lambda_1,\lambda_2)}(\mathbf{k}_1,\mathbf{k}_2) = e_y^{(\lambda_1)}(\mathbf{k}_1)e_z^{(\lambda_2)}(\mathbf{k}_2) + e_z^{(\lambda_1)}(\mathbf{k}_1)e_y^{(\lambda_2)}(\mathbf{k}_2),$$

$$g_{zx}^{(\lambda_1,\lambda_2)}(\mathbf{k}_1,\mathbf{k}_2) = e_z^{(\lambda_1)}(\mathbf{k}_1)e_x^{(\lambda_2)}(\mathbf{k}_2) + e_x^{(\lambda_1)}(\mathbf{k}_1)e_z^{(\lambda_2)}(\mathbf{k}_2), \tag{5}$$

where $\mathbf{e}^{(1)}(\mathbf{k})$ and $\mathbf{e}^{(2)}(\mathbf{k})$ are the two linearly independent polarization vectors of the electromagnetic field with wave vector $\mathbf{k}$; they satisfy the condition $\mathbf{e}^{(1)}(\mathbf{k}) \times \mathbf{e}^{(1)}(\mathbf{k}) = \mathbf{k}/|\mathbf{k}|$.

In Hamiltonian (4) the linear polariton effect is not taken into account since, for the process under investigation, the two polaritons that belong to the photonlike component of the lower polariton branch lead to the excitation of polaritons at the bottom of the upper polariton branch, which is the excitonlike one in the given spectral range $\omega_{ph}(\mathbf{k}) \approx \omega_{ex}(\mathbf{0})/2$.

Using assumptions (iii) and (iv), we obtain from Eq. (4) the following equations for the macroscopic exciton and photon amplitudes $a_\alpha(\mathbf{k},t) = \langle \hat{a}_\alpha(\mathbf{k}) \rangle_t$ and $c_\lambda(\mathbf{k},t) = \langle \hat{c}_\lambda(\mathbf{k}) \rangle_t$:

$$\left[i\hbar\frac{d}{dt} - \hbar\omega_{ex}(\mathbf{k}) + i\Gamma_{ex} \right] a_\alpha(\mathbf{k},t) = \frac{1}{2!\sqrt{V}} \sum_{\mathbf{k}'} \sum_{\lambda_1,\lambda_2=1,2} g_\alpha^{(\lambda_1,\lambda_2)} \times (\mathbf{k}', \mathbf{k}-\mathbf{k}') c_{\lambda_1}(\mathbf{k}',t) c_{\lambda_2}(\mathbf{k}-\mathbf{k}',t), \tag{6}$$

$$\left[i\hbar\frac{d}{dt} - \hbar\omega_{ph}(\mathbf{k}) + i\Gamma_{ph} \right] c_\lambda(\mathbf{k},t) = \frac{1}{\sqrt{V}} \sum_{\mathbf{k}'} \sum_{\alpha=xy,yz,zx} \sum_{\lambda'=1,2} g_\alpha^{(\lambda,\lambda')} \times (\mathbf{k},\mathbf{k}') a_\alpha(\mathbf{k}+\mathbf{k}',t) c_{\lambda'}^*(\mathbf{k}',t) + j_\lambda(\mathbf{k},t). \tag{7}$$

The photon amplitudes can be expressed as the sum of two terms

$$c_\lambda(\mathbf{k},t) = c_\lambda^p(\mathbf{k},t) + \bar{c}_\lambda(\mathbf{k},t). \tag{8}$$

The former, $c_\lambda^p(\mathbf{k},t)$, satisfies the equation

$$\left[i\hbar\frac{d}{dt} - \hbar\omega_{ph}(\mathbf{k}) + i\Gamma_{ph} \right] c_\lambda^p(\mathbf{k},t) = j_\lambda(\mathbf{k},t) \tag{9}$$

and can be written as

$$c_\lambda^p(\mathbf{k},t) = \sqrt{V}\delta_{\lambda,1}[(\delta_{\mathbf{k},\mathbf{k}_1}e^{i\varphi_{\mathbf{k}_1}} + \delta_{\mathbf{k},\mathbf{k}_3}e^{i\varphi_{\mathbf{k}_3}})C(t) + \delta_{\mathbf{k},\mathbf{k}_2}e^{i\varphi_{\mathbf{k}_2}}C(t-t_d)]e^{-i\omega_0 t}, \tag{10}$$

here V is the electromagnetic field quantization volume ($V \to \infty$); $\mathbf{k}_1$, $\mathbf{k}_3$, and $\mathbf{k}_2$ are, respectively, the wave vectors of the two pump pulses and the probe pulse; $\varphi_{\mathbf{k}_1}$, $\varphi_{\mathbf{k}_3}$, and $\varphi_{\mathbf{k}_2}$ are their initial phases; $t_d \geq 0$ is the delay time between the pump pulses and the probe pulse; and $\omega_0 = \omega_{ph}(\mathbf{k}_1)$ and $C(t)$ are the carrier frequency and the envelope of each of the three pulses. We will assume $C(t)$ to be a specified function of time.

The amplitude $\bar{c}_\lambda(\mathbf{k},t)$ of the secondary electromagnetic field due to the polarization of the medium obeys the equation

$$\left[i\hbar\frac{d}{dt}-\hbar\omega_{ph}(\mathbf{k})+i\Gamma_{ph}\right]\bar{c}_\lambda(\mathbf{k},t)=\frac{1}{\sqrt{V}}\sum_{\mathbf{k}'}\sum_{\alpha=xy,yz,zx}\sum_{\lambda'=1,2}g_\alpha^{(\lambda,\lambda')}\times(\mathbf{k},\mathbf{k}')a_\alpha(\mathbf{k}+\mathbf{k}',t)c_{\lambda'}^*(\mathbf{k}',t). \quad (11)$$

It follows from Eq. (11) that $\bar{c}_\lambda(\mathbf{k},t)\neq 0$ only when excitons are present in the system.

III. SPECIFIC CONFIGURATION OF THE EXPERIMENT

We now consider a configuration in which the equations for the amplitudes $\bar{c}_\lambda(\mathbf{k},t)$ and $a_\alpha(\mathbf{k},t)$ have the simplest form. We choose the polarizations vectors of the counterpropagating pump waves to be orthogonal to each other and assume that the polarization vector of the probe wave coincides with the polarization vector of one of the pump waves,

$$\mathbf{k}_3=-\mathbf{k}_1=\frac{\sqrt{\varepsilon_b}\omega_0}{c}\hat{\mathbf{y}},\quad \mathbf{k}_2=\frac{\sqrt{\varepsilon_b}\omega_0}{c}(\hat{\mathbf{x}}\sin\Theta+\hat{\mathbf{y}}\cos\Theta), \quad (12)$$

$$\mathbf{e}^{(1)}(\mathbf{k}_1)=\hat{\mathbf{z}},\quad \mathbf{e}^{(2)}(\mathbf{k}_1)=-\hat{\mathbf{x}}, \quad (13)$$

$$\mathbf{e}^{(1)}(\mathbf{k}_2)=\hat{\mathbf{z}},\quad \mathbf{e}^{(2)}(\mathbf{k}_2)=\hat{\mathbf{x}}\cos\Theta-\hat{\mathbf{y}}\sin\Theta, \quad (14)$$

$$\mathbf{e}^{(1)}(\mathbf{k}_3)=\hat{\mathbf{x}},\quad \mathbf{e}^{(2)}(\mathbf{k}_3)=-\hat{\mathbf{z}}, \quad (15)$$

where $\hat{\mathbf{x}}$, $\hat{\mathbf{y}}$, and $\hat{\mathbf{z}}$ are the unit vectors defining the Cartesian coordinate system.

Let us investigate which excitons and secondary photons are generated in the system under the action of the external field represented by Eq. (10). Here we consider only the case of very small values of the angle Θ, so $\cos\Theta\approx 1$. If we substitute the amplitudes [Eq. (10)] into the right-hand side of Eq. (6), instead of the amplitudes $c_\lambda(\mathbf{k},t)$, we see that the external field creates only excitons with amplitudes $a_{zx}(\mathbf{0},t)$ and $a_\alpha(\mathbf{k}_2+\mathbf{k}_3,t)$.

We next substitute Eq. (10) into the right-hand side of Eq. (11) taking into account that only the exciton amplitudes $a_{zx}(\mathbf{0},t)$ and $a_\alpha(\mathbf{k}_2+\mathbf{k}_3,t)$ differ from zero. We can then see that (i) the waves with the wave vectors $\mathbf{k}_1$, $\mathbf{k}_3$, and $\mathbf{k}_2$ are, in turn, influenced by the excitons that they generate $[c_\lambda(\mathbf{k}_i,t), i=1,2,3]$ and (ii) additional electromagnetic waves with the amplitudes $c_1(-\mathbf{k}_2,t)$ and $c_1(\mathbf{k}_2+2\mathbf{k}_3,t)$ are excited.

For the wave with amplitude $c_1(\mathbf{k}_2+2\mathbf{k}_3,t)$ the dimensionless resonance detuning

$$\delta_{ph}(\mathbf{k})=\frac{\omega_{ph}(\mathbf{k})}{\omega_0}-1 \quad (16)$$

is given as $\delta_{ph}(\mathbf{k}_2+2\mathbf{k}_3)=\sqrt{5+4\cos\Theta}-1$. Therefore for oblique Θ the excitation of these waves is not resonant and can be neglected.

Using Eq. (6) it follows that the presence of an additional electromagnetic wave with amplitude $c_1(\mathbf{k}_4,t)[\mathbf{k}_4=-\mathbf{k}_2,\ \mathbf{e}^{(1)}(\mathbf{k}_4)=\hat{\mathbf{x}}\cos\Theta-\hat{\mathbf{y}}\sin\Theta,\ \mathbf{e}^{(2)}(\mathbf{k}_4)=\hat{\mathbf{z}}]$ leads to the creation of excitons with amplitudes $a_{zx}(\mathbf{0},t)$, $a_{zx}(\mathbf{k}_2+\mathbf{k}_3,t)$, $a_{zx}(\mathbf{k}_1+\mathbf{k}_4,t)$ and $a_{xy}(2\mathbf{k}_4,t)$, $a_{xy}(\mathbf{k}_3+\mathbf{k}_4,t)$, $a_{yz}(\mathbf{k}_1+\mathbf{k}_4,t)$, $a_{yz}(\mathbf{0},t)$. The right-hand side of the equations for the amplitudes $a_{xy}(2\mathbf{k}_4,t)$, $a_{xy}(\mathbf{k}_3+\mathbf{k}_4,t)$, $a_{yz}(\mathbf{k}_1+\mathbf{k}_4,t)$, and $a_{yz}(\mathbf{0},t)$ is proportional to $\sin\Theta$. Hence, for rather small values of the angle Θ we can neglect the influence of these excitons on the system dynamics.

From Eq. (11) we find that the presence of excitons and photons with amplitudes $a_{zx}(\mathbf{0},t)$, $a_{zx}(\mathbf{k}_2+\mathbf{k}_3,t)$, $a_{zx}(\mathbf{k}_1+\mathbf{k}_4,t)$ and $c_1(\mathbf{k}_1,t)$, $c_1(\mathbf{k}_2,t)$, $c_1(\mathbf{k}_3,t)$, $c_1(\mathbf{k}_4,t)$ in turn leads to the generation of photons with amplitudes $c_1(\mathbf{k}_3+2\mathbf{k}_2,t)$, $c_1(\mathbf{k}_1+2\mathbf{k}_4,t)$, $c_1(\mathbf{k}_4+2\mathbf{k}_1,t)$, and $c_1(\mathbf{k}_2+2\mathbf{k}_3,t)$. But their generation is again not resonant and can be neglected.

From the above it follows that the dynamics of the system is described by the amplitudes $a_{zx}(\mathbf{0},t)$, $a_{zx}(\mathbf{k}_2+\mathbf{k}_3,t)$, $a_{zx}(\mathbf{k}_1+\mathbf{k}_4,t)$ and $c_1(\mathbf{k}_1,t)$, $c_1(\mathbf{k}_2,t)$, $c_1(\mathbf{k}_3,t)$, $c_1(\mathbf{k}_4,t)$. The relevant equations have the form

$$\left[i\hbar\frac{d}{dt}-\hbar\omega_{ex}(\mathbf{0})+i\Gamma_{ex}\right]a_{zx}(\mathbf{0},t)=\frac{g}{\sqrt{V}}[c_1(\mathbf{k}_1,t)c_1(\mathbf{k}_3,t)+c_1(\mathbf{k}_2,t)\bar{c}_1(\mathbf{k}_4,t)],$$

$$\left[i\hbar\frac{d}{dt}-\hbar\omega_{ex}(\mathbf{k}_1+\mathbf{k}_4)+i\Gamma_{ex}\right]a_{zx}(\mathbf{k}_1+\mathbf{k}_4,t)=\frac{g}{\sqrt{V}}c_1(\mathbf{k}_1,t)\bar{c}_1(\mathbf{k}_4,t),$$

$$\left[i\hbar\frac{d}{dt}-\hbar\omega_{ex}(\mathbf{k}_2+\mathbf{k}_3)+i\Gamma_{ex}\right]a_{zx}(\mathbf{k}_2+\mathbf{k}_3,t)=\frac{g}{\sqrt{V}}c_1(\mathbf{k}_2,t)c_1(\mathbf{k}_3,t),$$

$$\left[i\hbar\frac{d}{dt}-\hbar\omega_{ph}(\mathbf{k}_1)+i\Gamma_{ph}\right]\bar{c}_1(\mathbf{k}_1,t)=\frac{g}{\sqrt{V}}[a_{zx}(\mathbf{0},t)c_1^*(\mathbf{k}_3,t)+a_{zx}(\mathbf{k}_1+\mathbf{k}_4,t)\bar{c}_1^*(\mathbf{k}_4,t)],$$

$$\left[i\hbar\frac{d}{dt}-\hbar\omega_{ph}(\mathbf{k}_2)+i\Gamma_{ph}\right]\bar{c}_1(\mathbf{k}_2,t)=\frac{g}{\sqrt{V}}[a_{zx}(\mathbf{0},t)\bar{c}_1^*(\mathbf{k}_4,t)+a_{zx}(\mathbf{k}_2+\mathbf{k}_3,t)c_1^*(\mathbf{k}_3,t)],$$

$$\left[i\hbar\frac{d}{dt} - \hbar\omega_{ph}(\mathbf{k}_3) + i\Gamma_{ph} \right] \bar{c}_1(\mathbf{k}_3,t) = \frac{g}{\sqrt{V}}[a_{zx}(\mathbf{0},t)c_1^*(\mathbf{k}_1,t) + a_{zx}(\mathbf{k}_2+\mathbf{k}_3,t)c_1^*(\mathbf{k}_2,t)],$$

$$\left[i\hbar\frac{d}{dt} - \hbar\omega_{ph}(\mathbf{k}_4) + i\Gamma_{ph} \right] \bar{c}_1(\mathbf{k}_4,t) = \frac{g}{\sqrt{V}}[a_{zx}(\mathbf{0},t)c_1^*(\mathbf{k}_2,t) + a_{zx}(\mathbf{k}_1+\mathbf{k}_4,t)c_1^*(\mathbf{k}_1,t)], \tag{17}$$

where

$$c_1(\mathbf{k}_i,t) = \sqrt{V}C(t)e^{-i\omega_0 t + i\varphi_{\mathbf{k}_i}} + \bar{c}_1(\mathbf{k}_i,t), \quad (i=1,3),$$

$$c_1(\mathbf{k}_2,t) = \sqrt{V}C(t-t_d)e^{-i\omega_0 t + i\varphi_{\mathbf{k}_2}} + \bar{c}_1(\mathbf{k}_2,t),$$

$$c_1(\mathbf{k}_4,t) = \bar{c}_1(\mathbf{k}_4,t). \tag{18}$$

Converting to new dynamical variables $\tilde{a}(\mathbf{k},t)$ and $\tilde{c}(\mathbf{k},t)$ via the transformations

$$a_{zx}(\mathbf{0},t) = \sqrt{V}\frac{C^2(t_0)}{|C(t_0)|}e^{-2i\omega_0 t + i(\varphi_{\mathbf{k}_1}+\varphi_{\mathbf{k}_3})}\tilde{a}(\mathbf{0},t),$$

$$a_{zx}(\mathbf{k}_1+\mathbf{k}_4,t) = \sqrt{V}\frac{C^2(t_0)}{|C(t_0)|}e^{-2i\omega_0 t + i(2\varphi_{\mathbf{k}_1}+\varphi_{\mathbf{k}_3}-\varphi_{\mathbf{k}_2})}\tilde{a}(\mathbf{k}_1+\mathbf{k}_4,t),$$

$$a_{zx}(\mathbf{k}_2+\mathbf{k}_3,t) = \sqrt{V}\frac{C^2(t_0)}{|C(t_0)|}e^{-2i\omega_0 t + i(\varphi_{\mathbf{k}_2}+\varphi_{\mathbf{k}_3})}\tilde{a}(\mathbf{k}_2+\mathbf{k}_3,t),$$

$$c_1(\mathbf{k}_i,t) = \sqrt{V}C(t_0)e^{-i\omega_0 t + i\varphi_{\mathbf{k}_i}}\tilde{c}(\mathbf{k}_i,t), \quad (i=1,2,3),$$

$$\bar{c}_1(\mathbf{k}_4,t) = \sqrt{V}C(t_0)e^{-i\omega_0 t + i(\varphi_{\mathbf{k}_1}+\varphi_{\mathbf{k}_3}-\varphi_{\mathbf{k}_2})}\tilde{c}(\mathbf{k}_4,t) \tag{19}$$

and introducing the dimensionless parameters

$$\bar{t} = \omega_0 t, \quad \gamma_{ex} = \frac{\Gamma_{ex}}{\hbar\omega_0}, \quad \gamma_{ph} = \frac{\Gamma_{ph}}{\hbar\omega_0}, \quad \delta_{ex}(\mathbf{k}) = \frac{\omega_{ex}(\mathbf{k})}{\omega_0} - 2, \quad \xi = \frac{g\sqrt{|C(t_0)|^2}}{\hbar\omega_0} \ll 1, \tag{20}$$

we can rewrite the set of Eq. (17) in the form

$$\left[i\frac{d}{d\bar{t}} - \delta_{ex}(\mathbf{0}) + i\gamma_{ex} \right] \tilde{a}(\mathbf{0},\bar{t}) = \xi\{[f(\bar{t}) + \tilde{c}(\mathbf{k}_1,\bar{t})][f(\bar{t}) + \tilde{c}(\mathbf{k}_3,\bar{t})] + [f(\bar{t}-\bar{t}_d) + \tilde{c}(\mathbf{k}_2,\bar{t})]\tilde{c}(\mathbf{k}_4,\bar{t})\},$$

$$\left[i\frac{d}{d\bar{t}} - \delta_{ex}(\mathbf{0}) + i\gamma_{ex} \right] \tilde{a}(\mathbf{k}_1+\mathbf{k}_4,\bar{t}) = \xi[f(\bar{t}) + \tilde{c}(\mathbf{k}_1,\bar{t})]\tilde{c}(\mathbf{k}_4,\bar{t}),$$

$$\left[i\frac{d}{d\bar{t}} - \delta_{ex}(\mathbf{0}) + i\gamma_{ex} \right] \tilde{a}(\mathbf{k}_2+\mathbf{k}_3,\bar{t}) = \xi[f(\bar{t}-\bar{t}_d) + \tilde{c}(\mathbf{k}_2,\bar{t})][f(\bar{t}) + \tilde{c}(\mathbf{k}_3,\bar{t})],$$

$$\left(i\frac{d}{d\bar{t}} + i\gamma_{ph} \right) \tilde{c}(\mathbf{k}_1,\bar{t}) = \xi\{\tilde{a}(\mathbf{0},\bar{t})[f(\bar{t}) + \tilde{c}(\mathbf{k}_3,\bar{t})]^* + \tilde{a}(\mathbf{k}_1+\mathbf{k}_4,\bar{t})\tilde{c}^*(\mathbf{k}_4,\bar{t})\},$$

$$\left(i\frac{d}{d\bar{t}} + i\gamma_{ph} \right) \tilde{c}(\mathbf{k}_2,\bar{t}) = \xi[\tilde{a}(\mathbf{0},\bar{t})\tilde{c}^*(\mathbf{k}_4,\bar{t}) + \tilde{a}(\mathbf{k}_2+\mathbf{k}_3,\bar{t})\tilde{c}^*(\mathbf{k}_3,\bar{t})],$$

$$\left(i\frac{d}{d\bar{t}} + i\gamma_{ph} \right) \tilde{c}(\mathbf{k}_3,\bar{t}) = \xi\{\tilde{a}(\mathbf{0},\bar{t})[f(\bar{t}) + \tilde{c}(\mathbf{k}_1,\bar{t})]^* + \tilde{a}(\mathbf{k}_2+\mathbf{k}_3,\bar{t})[f(\bar{t}-\bar{t}_d) + \tilde{c}(\mathbf{k}_2,\bar{t})]^*\},$$

$$\left(i\frac{d}{d\bar{t}}+i\gamma_{ph}\right)\tilde{c}(\mathbf{k}_4,\bar{t})=\xi\{\tilde{a}(\mathbf{0},\bar{t})[f(\bar{t}-\bar{t}_d)+\tilde{c}(\mathbf{k}_2,\bar{t})]^*+\tilde{a}(\mathbf{k}_1+\mathbf{k}_4,\bar{t})[f(\bar{t})+\tilde{c}(\mathbf{k}_1,\bar{t})]^*\}. \quad (21)$$

Here $f(t)=C(t)/C(t_0)$ and the time t_0 will be defined later. In deriving the set of Eq. (21) we have used the fact that the dimensionless resonance detunings $\delta_{ex}(\mathbf{k}_1+\mathbf{k}_4)$ and $\delta_{ex}(\mathbf{k}_2+\mathbf{k}_3)$ can be written in the form

$$\delta_{ex}(\mathbf{k}_1+\mathbf{k}_4)=\delta_{ex}(\mathbf{k}_2+\mathbf{k}_3)=\delta+\varepsilon_b\frac{\hbar\omega_0}{m_{ex}c^2}\sin^2\frac{\Theta}{2},$$

$$\delta=\frac{\omega_{ex}(\mathbf{0})}{\omega_0}-2. \quad (22)$$

For Cu_2O the parameter $\varepsilon_b\hbar\omega_0/m_{ex}c^2\ll\xi$, so in what follows we will assume $\delta_{ex}(\mathbf{k}_1+\mathbf{k}_4)=\delta_{ex}(\mathbf{k}_2+\mathbf{k}_3)\approx\delta\ll 1$.

IV. EXTERNAL FIELD APPROXIMATION

The complete set of nonlinear Eq. (21), taking into account the reaction of the excitons on the electromagnetic waves that generate them, can be only solved using numerical methods. Hence it is desirable to obtain simpler equations, which can be solved analytically but do not supply as detailed a description of the temporal evolution of the system. This allowed a deeper insight into the physics of the processes which occur in the system.

Now when the inequality

$$\xi\sqrt{|\tilde{a}(\mathbf{0},\bar{t})|^2}\ll\gamma_{ph} \quad (23)$$

is fulfilled, the photons generated leave the system before they can influence the excitons, and the second summation in Eq. (21) and expressions of the type $[f(\bar{t})+\tilde{c}(\mathbf{k}_i,\bar{t})]$, $i=1,2,3$ can be neglected. Our system of equations then takes the form

$$\left(i\frac{d}{d\bar{t}}-\delta+i\gamma_{ex}\right)\tilde{a}(\mathbf{0},\bar{t})=\xi[f^2(\bar{t})+f(\bar{t}-\bar{t}_d)\tilde{c}(\mathbf{k}_4,\bar{t})], \quad (24)$$

$$\left(i\frac{d}{d\bar{t}}-\delta_{ex}+i\gamma_{ex}\right)\tilde{a}(\mathbf{k}_1+\mathbf{k}_4,\bar{t})=\xi f(\bar{t})\tilde{c}(\mathbf{k}_4,\bar{t}), \quad (25)$$

$$\left(i\frac{d}{d\bar{t}}+i\gamma_{ph}\right)\tilde{c}(\mathbf{k}_4,\bar{t})=\xi[\tilde{a}(\mathbf{0},\bar{t})f^*(\bar{t}-\bar{t}_d)+\tilde{a}(\mathbf{k}_1+\mathbf{k}_4,\bar{t})\tilde{c}^*(\mathbf{k}_1,\bar{t})], \quad (26)$$

where only the three important equations are shown.

With the same degree of accuracy, the right-hand side in Eq. (25) and the second term in the square brackets on the right-hand side of Eq. (24), associated with the influence of the newly generated photons on the excitons, can be neglected. As a result, we obtain a simple system of linear equations

$$\begin{cases}\left(i\frac{d}{d\bar{t}}-\delta+i\gamma_{ex}\right)\tilde{a}(\mathbf{0},\bar{t})=\xi f^2(\bar{t}),\\ \left(i\frac{d}{d\bar{t}}+i\gamma_{ph}\right)\tilde{c}(\mathbf{k}_4,\bar{t})=\xi\tilde{a}(\mathbf{0},\bar{t})f^*(\bar{t}-\bar{t}_d),\end{cases} \quad (27)$$

which have a clear physical meaning: the first equation describes the generation of excitons by the two pump pulses 1 and 3 while the second equation describes the generation of the resultant signal 4 by the probe pulse 2 and the newly generated excitons. In this approximation all three incident pulses are treated as *specified external fields*. The validity of the approximations assuming that inequality Eq. (23) is fulfilled will be further confirmed by the numerical calculations.

Let us solve Eq. (27) for bell-shaped pulses with a maximum at $\bar{t}=\bar{t}_0$. We assume that the pulse duration $\bar{t}_p$ satisfies the following inequalities:

$$\gamma_{ph}^{-1}\ll\bar{t}_p\ll\gamma_{ex}^{-1} \quad (28)$$

and the time $\bar{t}_0$ is chosen so that $\bar{t}_p\ll\bar{t}_0$. The first of inequalities in Eq. (28) is a necessary condition for the temporal description of the system that we use here. This implies that the duration of the pulse t_p, which propagates through the crystal with velocity $c/\sqrt{\varepsilon_b}$ is much greater than the time of flight of the photons through the crystal $\sqrt{\varepsilon_b}L/c$. In this case, the pulse spatial extension $ct_p/\sqrt{\varepsilon_b}$ significantly exceeds the sample thickness L. The fulfillment of the second inequality in Eq. (28) is necessary because it gives the possibility to probe the exciton condensate as a function of time and in this way monitor its temporal evolution.

Taking into account the first of the inequalities in Eq. (28) and the resonance condition

$$\delta t_p\ll 1, \quad (29)$$

we have from the first equation in Eq. (27)

$$\tilde{a}(\mathbf{0},\bar{t})=-i\xi\exp[-(\gamma_{ex}+i\delta)\bar{t}]\int_0^{\bar{t}}d\bar{t}_1\exp[(\gamma_{ex}+i\delta)\bar{t}_1]f^2(\bar{t}_1)$$

$$\approx-i\xi\sigma(\bar{t})\exp[-(\gamma_{ex}+i\delta)(\bar{t}-\bar{t}_0)], \quad (30)$$

where

$$\sigma(\bar{t})=\int_0^{\bar{t}}d\bar{t}_1 f^2(\bar{t}_1). \quad (31)$$

The function $\sigma(0)=0$ and increases monotonically with the increasing of $\bar{t}$. There is an inflection point at $\bar{t}=\bar{t}_0$ and on passing through it the function increases more slowly, changing little for $\bar{t}\gg\bar{t}_p$. Thus, the average density of excitons with the wave vector $\mathbf{k}=\mathbf{0}$,

$$n_{ex}(\mathbf{0},\bar{t}) = \frac{|a_{zx}(\mathbf{0},\bar{t})|^2}{V} = \xi^2 |C(t_0)|^2 \sigma^2(\bar{t}) \exp[-2\gamma_{ex}(\bar{t}-\bar{t}_0)] \tag{32}$$

sharply increases in the time interval from $\bar{t}$ to $\bar{t} \sim \bar{t}_p$ and then decreases exponentially.

Using Eq. (30), we can rewrite equation Eq. (23) in the form $\xi^2 \sigma(+\infty) \ll \gamma_{ph}$. Taking into account that $\sigma(+\infty) \sim \bar{t}_p$, we find

$$\xi^2 \bar{t}_p \ll \gamma_{ph}. \tag{33}$$

We now use the second equation in Eq. (27). Taking into account the second inequality in Eq. (28), we sequentially find

$$\tilde{c}(\mathbf{k}_4,\bar{t}) \approx -i\xi \int_0^{\bar{t}} d\tau \exp(-\gamma_{ph}\tau) \tilde{a}(\mathbf{0},\bar{t}-\tau) f(\bar{t}-\bar{t}_d-\tau). \tag{34}$$

The truncating multiplier $\exp(-\gamma_{ph}\tau)$ in Eq. (34) restricts the integration over the variable τ to the range from 0 to the value $\sim \gamma_{ph}^{-1}$. The typical scale for the variation in the function $f(\bar{t})$ is $\bar{t}_p$ while that for the function $\tilde{a}(\mathbf{0},\bar{t})$ is $\sim \gamma_{ex}^{-1}$ (for $\bar{t} \gg \bar{t}_p$). Then, when the inequalities in Eq. (28) are fulfilled, we can neglect the variation in these functions over the specified integration interval and obtain

$$\begin{aligned}\tilde{c}(\mathbf{k}_4,\bar{t}) &\approx -i\xi\tilde{a}(\mathbf{0},\bar{t}) f(\bar{t}-\bar{t}_d) \int_0^{\bar{t}} d\tau \exp(-\gamma_{ph}\tau) \\ &\approx -i\xi\tilde{a}(\mathbf{0},\bar{t}) f(\bar{t}-\bar{t}_d) \frac{1-\exp(-\gamma_{ph}\bar{t})}{\gamma_{ph}} \\ &\approx -i\xi\tilde{a}(\mathbf{0},\bar{t}_0+\bar{t}_d) f(\bar{t}-\bar{t}_d) \gamma_{ph}^{-1}. \end{aligned} \tag{35}$$

For the average density of the radiated photons we obtain

$$n_{ph}(\mathbf{k}_4,\bar{t}) = \frac{\xi^2}{\gamma_{ph}^2} n_{ex}(\mathbf{0},\bar{t}_0+\bar{t}_d) f^2(\bar{t}-\bar{t}_d). \tag{36}$$

Equation (36) was derived in such a way that it is also valid for a case where the decay of the exciton condensate is nonexponential in character. In this case it is sufficient that the excitonic amplitude not experience significant changes during a time interval $\sim \gamma_{ph}^{-1}$,

$$\frac{d}{d\bar{t}} \tilde{a}(\mathbf{0},\bar{t}) \ll \gamma_{ph} \tilde{a}(\mathbf{0},\bar{t}).$$

It is seen from Eq. (36) that the density of radiated photons $n_{ph}(\mathbf{k}_4,\bar{t})$ exhibits the same dependence on the time $\bar{t}$, as the density of photons in the probe pulse. The maximal value of $n_{ph}(\mathbf{k}_4,\bar{t})$ is reached for $\bar{t}=\bar{t}_0+\bar{t}_d$ and is given by

$$n_{ph}(\mathbf{k}_4,\bar{t}_0+\bar{t}_d) = \frac{\xi^4}{\gamma_{ph}^2} |C(t_0)|^2 \sigma^2(\bar{t}_0+\bar{t}_d) \exp(-2\gamma_{ex}\bar{t}_d). \tag{37}$$

It follows from Eq. (37) that for $\bar{t}_d \gg \bar{t}_p$, the probe and pump pulses are separated in time, and the dependence of the maximal value of $n_{ph}(\mathbf{k}_4,\bar{t})$ on the delay time $\bar{t}_d$ has the same shape as the $\bar{t}$ dependence of the density of excitons, $n_{ex}(\mathbf{0},\bar{t})$. Therefore, by investigating the dependence of the resultant four-wave-mixing signal on $\bar{t}_d$, one can obtain information about the temporal evolution of the exciton condensate. However, this signal is weak since the interaction constant for the two-photon generation of excitons from the crystal ground state is small; so it may be difficult to observe it experimentally. One can also study the time-integrated signal, whose value can be increased as a result of multiple repetitions of the experiment over time intervals $\gtrsim \gamma_{ex}^{-1}$.

The density of photons radiated during the time of the experiment is

$$\begin{aligned} N(t_d) &= \int_0^{+\infty} dt n_{ph}(\mathbf{k}_4,t) = \frac{\xi^2}{\gamma_{ph}^2} n_{ex}(\mathbf{0},\bar{t}_0+\bar{t}_d) \int_0^{+\infty} dt f^2(\bar{t}-\bar{t}_d) \\ &= \frac{\xi^2 \sigma(+\infty)}{\gamma_{ph}^2} n_{ex}(\mathbf{0},\bar{t}_0+\bar{t}_d). \end{aligned} \tag{38}$$

Substituting Eq. (32) into Eq. (38), we obtain

$$N(t_d) = \frac{\xi^4 |C(t_0)|^2 \sigma(+\infty) \sigma^2(\bar{t}_0+\bar{t}_d)}{\gamma_{ph}^2} \exp(-2\gamma_{ex}\bar{t}_d). \tag{39}$$

For $\bar{t}_d \gg \bar{t}_p$,

$$N(t_d) = \frac{\xi^4 |C(t_0)|^2 \sigma^3(+\infty)}{\gamma_{ph}^2} \exp(-2\gamma_{ex}\bar{t}_d). \tag{40}$$

We see that one can also obtain information about the temporal evolution of the exciton condensate via the study of the dependence of time-integrated four-wave-mixing signal on the delay time $\bar{t}_d$ between the probe and the pump pulses.

Returning to our initial notation, we can see that the time-integrated signal [Eq. (40)] is proportional to the areas

$$\int_0^{+\infty} dt |C(t)|^2$$

of all three incoming pulses.

Applying the above formulas for the case of Gaussian pulses

$$f(\bar{t}) = \exp\left[-2\frac{(\bar{t}-\bar{t}_0)^2}{\bar{t}_p^2}\right], \tag{41}$$

we obtain

$$\begin{aligned} \sigma(\bar{t}) &= \frac{\sqrt{\pi}\bar{t}_p}{4}\left\{\mathrm{erf}\left(2\frac{\bar{t}_0}{\bar{t}_p}\right) + \mathrm{erf}\left[2\frac{(\bar{t}-\bar{t}_0)}{\bar{t}_p}\right]\right\} \\ &\approx \frac{\sqrt{\pi}\bar{t}_p}{4}\left\{1 + \mathrm{erf}\left[2\frac{(\bar{t}-\bar{t}_0)}{\bar{t}_p}\right]\right\}. \end{aligned} \tag{42}$$

Hence,

$$n_{ex}(\mathbf{0},\bar{t}) = \pi\left(\frac{\xi\bar{t}_p}{4}\right)^2 |C(t_0)|^2 \left\{1 + \mathrm{erf}\left[2\frac{(\bar{t}-\bar{t}_0)}{\bar{t}_p}\right]\right\}^2 \times \exp[-2\gamma_{ex}(\bar{t}-\bar{t}_0)], \quad (43)$$

$$n_{ph}(\mathbf{k}_4,\bar{t}) = \pi\left(\frac{\xi^2\bar{t}_p}{4\gamma_{ph}}\right)^2 |C(t_0)|^2 \exp\left[-2\frac{(\bar{t}-\bar{t}_0-\bar{t}_d)^2}{\bar{t}_p^2}\right] \times \left[1 + \mathrm{erf}\left(2\frac{\bar{t}_d}{\bar{t}_p}\right)\right]^2 \exp(-2\gamma_{ex}\bar{t}_d), \quad (44)$$

$$N(t_d) = \frac{\sqrt{\pi^3}\xi^4\bar{t}_p^3}{4^3\gamma_{ph}^2}|C(t_0)|^2\left[1 + \mathrm{erf}\left(2\frac{\bar{t}_d}{\bar{t}_p}\right)\right]^2 \times \exp(-2\gamma_{ex}\bar{t}_d). \quad (45)$$

When inequality in Eq. (29) is fulfilled, the results obtained do not depend on the value of the resonance detuning, δ.

Note, that when the integral in Eq. (34) is calculated exactly, we obtain the following expression for the density of the radiated photons:

$$n_{ph}(\mathbf{k}_4,\bar{t}) = 2\pi^2\left(\frac{\xi\bar{t}_p}{4}\right)^4 |C(t_0)|^2\left[1 + \mathrm{erf}\left(2\frac{\bar{t}_d}{\bar{t}_p}\right)\right]^2 \exp(-2\gamma_{ex}\bar{t}_d) \times \left\{1 + \mathrm{erf}\left[\frac{\sqrt{2}\left(\bar{t}-\bar{t}_0-\bar{t}_d-\frac{\gamma_{ph}\bar{t}_p^2}{4}\right)}{\bar{t}_p}\right]\right\}^2 \exp\left\{-\gamma_{ph}\left[(\bar{t}-\bar{t}_0-\bar{t}_d)-\frac{\gamma_{ph}\bar{t}_p^2}{4}\right]\right\}. \quad (46)$$

The same results can be obtained also for the case of square pump and probe pulses for which the set of Eq. (27) can be solved exactly (see Appendix). These results obtained within the framework of the above restrictions have a clear physical interpretation. The counter-propagating pump pulses, denoted 1 and 3 in Fig. 1, create an excitonic condensate in the system. After their action has terminated, the condensate evolution is determined by the internal interactions in the system, which we have modeled as an exponential decay. If after some time t_d following the condensate formation, the system is subjected to the action of a probe pulse, 2, stimulated radiation, 4, traveling opposite to 2 is generated, the over all behavior being interpreted as a particular kind of four-wave-mixing process. The duration of the resulting signal is determined by the duration of the probe pulse t_p but most importantly its intensity is proportional to the density of the excitonic condensate. Since this density diminishes as $\exp(-2\gamma_{ex}\bar{t})$, it is clear that the later the application of the probe pulse on the excitonic condensate, the smaller the resulting signal 4. Thus, the duration of the resulting signal does not depend on the delay time t_d but its intensity will decrease exponentially with increasing t_d; i.e., the resulting time-integrated signal 4 should decay as $\exp(-2\gamma_{ex}\bar{t}_d)$.

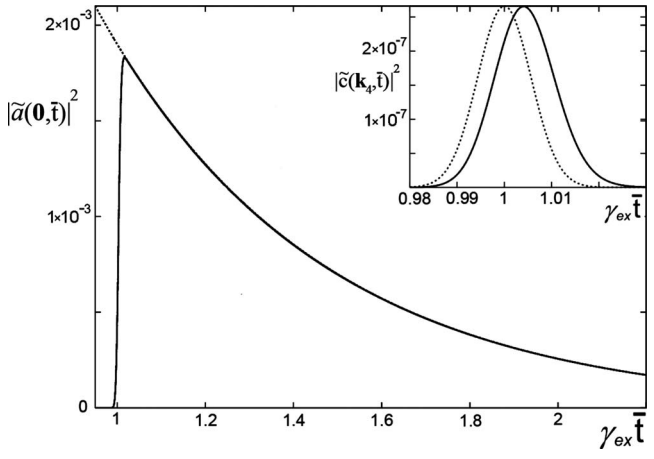

FIG. 2. The solid curve describes the temporal evolution of the relative density of the exciton condensate $|\tilde{a}(\mathbf{0},\bar{t})|^2 = n_{ex}(\mathbf{0},\bar{t})/|C(\bar{t}_0)|^2$ for $S=1$ MW/cm^2 and $t_d=10t_p$. The dotted curve describes the dependence $0.0019\exp(-2\gamma_{ex}\bar{t})$. Inset: the solid curve describes the temporal dependence of the relative density of generated photons $|\tilde{c}(\mathbf{k}_4,\bar{t})|^2 = n_{ph}(\mathbf{k}_4,\bar{t})/|C(\bar{t}_0)|^2$. The dotted curve shows the dependence $2.66\times10^{-7}f^2(\bar{t}-\bar{t}_d)$.

V. ESTIMATION OF INTERACTION CONSTANT

The four-wave-mixing phenomenon examined above results from the creation of excitons from the crystal ground state as a result of absorption of two cross-polarized photons of the same frequency $\omega_0 \approx (E_g - I_1)/2\hbar$, which propagate opposite directions; here E_g is the forbidden gap and I_1 is the ionization energy of the exciton ground state. Using Hamiltonian (2)–(4) one obtains the following expression for the transition probability per unit time:

$$W = \frac{2\pi}{\hbar}\frac{g^2\bar{n}^2}{V}\delta(E_g - I_1 - 2\hbar\omega_0), \quad (47)$$

where $\bar{n}$ is an average number of photons in the initial state. On the other hand, the probability of the same process, calculated in Ref. 28 on the basis of an exciton as a coupled electron-hole pair has the form,

$$W = \frac{2\pi}{\hbar}\left(\frac{64\hbar^2 e^2 E_g}{3a_{ex}\mu v_0}\right)^2 \frac{2f_{2p}\bar{n}^2}{N\varepsilon_b^2\omega_0^2 m_0(E_g - I_2)}\left[\int_0^\infty \frac{dxx^4}{(x^2+1)\left(\frac{\hbar^2 x^2}{2\mu a_{ex}^2} + E_g - \hbar\omega_0\right)}\right.$$
$$\left. + 2\pi\sum_{n=2}^{\infty}\left(\frac{n^2-1}{n^5}\right)\left(\frac{n}{n+1}\right)^4\left(\frac{n-1}{n+1}\right)^{n-2}\left(\frac{1}{E_g - I_n - \hbar\omega_0}\right)\right]^2 \delta(E_g - I_1 - 2\hbar\omega_0). \quad (48)$$

Here I_n is the ionization energy of the nth exciton state, m_0 is the mass of the free electron, e is its charge, a_{ex} is the effective Bohr exciton radius, μ is its reduced mass, N is the total number of elementary cells in the crystal, v_0 is their volume, f_{2p} is the oscillator strength of the one-photon transition into the $2p$ state of the exciton. The integral and the sum in the square brackets in Eq. (48) take into account, respectively, both the band and exciton intermediate states associated with the same pair of bands involved in the formation of the final exciton state. The estimations performed in Ref. 28 show that for case of the Cu_2O crystal, the effect of the exciton intermediate Rydberg states on the transition amplitude is considerably less than that of the band intermediate states. Therefore, the sum in the square brackets in formula (48) can be omitted. Comparing Eqs. (47) and (48) and making a simple transformation we obtain the following expression for the interaction constant:

$$g \approx \frac{16}{3}\sqrt{f_{2p}}\hbar\Omega_p\sqrt{8\pi a_{ex}^3}\frac{1+2\sqrt{y}}{\sqrt{y}(1+\sqrt{y})^2},$$

$$y = \frac{E_g}{2I_1}, \quad I_1 = \frac{\mu e^4}{2\hbar^2\varepsilon_b^2}, \quad a_{ex} = \frac{\hbar^2\varepsilon_b}{\mu e^2}, \quad \Omega_p^2 = \frac{4\pi e^2}{m_0 v_0 \varepsilon_b}. \quad (49)$$

Assuming $E_g = 2.17$ eV, $I_1 = 150$ meV, $\mu = 0.56m_0$, $a_{ex} = 7$ Å, $\varepsilon_b = 6.5$, $v_0 = 0.77\times10^{-22}$ cm^2, $f_{2p} = 2\times10^{-6}$, where m_0 is the mass of the free electron, we find: $g \approx 3\times10^{-25}$ erg cm$^{3/2}$.

VI. NUMERICAL RESULTS AND DISCUSSIONS

In this section we present the results of the numerical investigation of the temporal evolution of the exciton condensate and the generated photon densities, as well as the dependence of the time-integrated phase-conjugated signal on the delay time between the probe and the pump pulses. We will compare these results with those obtained on the basis of the simplified set of Eq. (27) as well as those of the approximate solutions in Eqs. (43)–(46) of this set.

The following values of parameters were used for the numerical calculations: $\omega_0 = 1.545\times10^{15}$ s^{-1}, $\Gamma_{ex} = 1$ μeV, $L = 4\times10^{-2}$ cm, and $t_p = 15$ ps.

Let us first consider a case of small excitation levels, when the flux in the probe and pump pulses is $S = 1$ MW/cm^2. Figure 2 shows the time dependence of the density of the exciton condensate obtained as a result of the numerical solution to the full set of Eq. (21). Note that it accurately coincides with the dependence predicted by Eq. (43). Also note that Eq. (43) was obtained as a result of the approximate solution to the set of Eq. (27), where all three incident pulses were treated as given external fields. According to Fig. 2, the decay of the exciton condensate for $t \gg t_p$ exhibits an exponential behavior with the decay constant γ_{ex}.

The inset in Fig. 2 depicts the temporal dependence of the density of generated photons. The results obtained using the numerical integration of the full set of Eq. (21) and of the set of Eq. (27) that corresponds to the external field approximation coincide and are well described by Eq. (46). The resulting phase-conjugated signal exhibits the same form as a probe pulse; however, it is shifted to the right-hand side by an amount $\sim\gamma_{ex}^{-1}$ (i.e., there is a small delay by a time of order the photon transit time through the crystal). This delay is absent in the approximate formula (44), which also leads to an overestimate of the photon density by a factor 1.3 compared with Eq. (46).

Figure 3 shows the dependence of the resulting time-integrated signal as a function of the delay time $\bar{t}_d$. The numerical solutions to the set of Eq. (27), which correspond to the external field approximation, again coincide with the re-

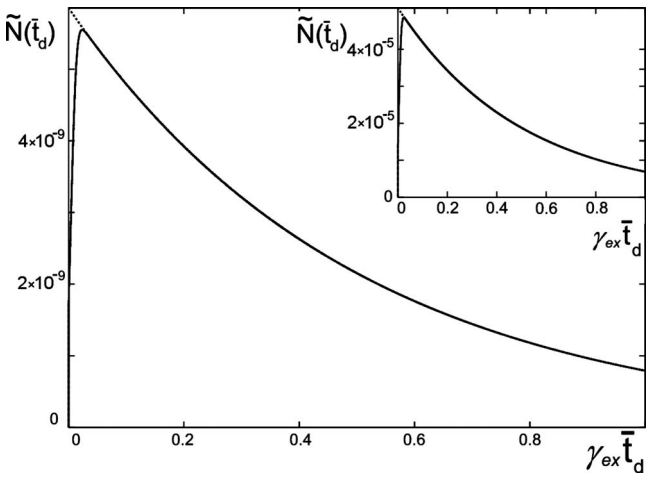

FIG. 3. The solid curve describes the $\tilde{N}(\bar{t}_d)$ dependence ($\tilde{N}(\bar{t}_d) = \gamma_{ex}\omega_0 N(\bar{t}_d)/|C(\bar{t}_0)|^2$) for $S = 1$ MW/cm^2 while dotted curve shows the form $7.9\times10^{-10}\exp(-2\gamma_{ex}\bar{t}_d)$. The solid curve in the inset describes the dependence $\tilde{N}(\bar{t}_d)$ for $S = 100$ MW/cm^2 while the dotted curve shows the form $6.9\times10^{-6}\exp(-2\gamma_{ex}\bar{t}_d)$.

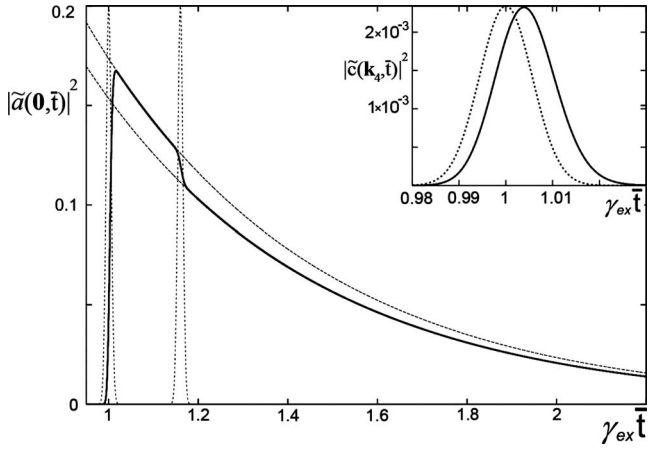

FIG. 4. The solid curve describes the temporal evolution of the relative density of the exciton condensate for $S=100$ MW/cm^2 and $t_d=10t_p$ while the dashed curves show dependences $0.1535\exp(-2\gamma_{ex}\bar{t})$ and $0.1735\exp(-2\gamma_{ex}\bar{t})$. The dotted curve shows the probe and pump pulses. The solid curve in the inset describes the temporal evolution of the relative density of the phase-conjugated photons generated while the dotted line shows the dependence $2.34\times10^{-3}f^2(\bar{t}-\bar{t}_d)$.

sults obtained from solving the complete set of Eq. (21). The approximate form (45) for the time-integrated signal when $t_d \gg t_p$ is only lager by a factor 1.16. The dependence of $N(t_d)$ for $t_d \gg t_p$ exhibits an exponential behavior with the decay constant γ_{ex}. Clearly, the external field approximation is quite satisfactory for the chosen intensities of the probe and pump pulses. A minor difference of the approximate formulas (44) and (46) from the results obtained via numerical solution of the full set of Eq. (21) is related to the fact that the spatial extent of the pulse is only three times the crystal thickness; therefore, the first of the strict inequalities in Eq. (28) used to obtain Eq. (44) is not well satisfied. When the crystal thickness is an order of magnitude less than the spatial pulse width, Eqs. (43)–(45) should describe the temporal evolution of the system with great accuracy.

The aforementioned results do not qualitatively change if we increase the flux density of the incident pulses to $S=10$ MW/cm^2. For densities of $S=100$ MW/cm^2 and greater, Eq. (43) obtained in the external field approximation, rather well describes the temporal evolution of the density of the exciton condensate, which is generated only due to the pump pulses. However, formula (43) does not take into account the influence of the probe pulse on the exciton condensate.

According to Fig. 4, the condensate decay for $t \gg t_p$ initially occurs in an exponential fashion with the decay constant γ_{ex}. However, as a result of the probe pulse, a dramatic fall of the condensate density occurs during the time interval when the phase-conjugated signal is generated. When the action of the probe pulse is terminated, the subsequent exponential decay continues with the same decay constant, γ_{ex}. The greater the density of the photon flux in the probe pulse, the greater the drop in the exciton density that occurs during the time of its action. In other words, the resulting signal can be treated as being *stimulated by the probe pulse from the excitons generated by the pump pulses*.

According to the inset in Fig. 4, the resultant phase-conjugated signal 4 has approximately the same form as the probe pulse; however, it is delayed by a time of order $\sim\gamma_{ex}^{-1}$. The external field approximation in this case leads to signal which is overestimated by only a factor of 1.145 compared with that presented in Fig. 4. The numerical results found in this approximation agree well with the results predicted by Eq. (46). At the same time, Eq. (44) does not account the aforementioned shift of the maximum of the radiation peak; moreover, it overestimates the photon density by a factor of 1.5.

The inset in Fig. 3 shows that for $t_d \gg t_p$ the dependence of the time-integrated phase-conjugated signal on the delay time t_d exhibits an exponential fall with the decay constant γ_{ex}. According to Fig. 4, the probe pulse in the proposed experiment significantly influences the temporal evolution of excitons. Nevertheless, examination of the dependence $N(t_d)$ allows one to gather information related to the temporal evolution of the "free" exciton condensate, which is generated by the pump pulses when not perturbed by the probe pulse. Application of the external field approximation leads to a function $N(t_d)$, which overestimates those presented in the inset of Fig. 3 by only a factor 1.15. Using Eq. (45) overestimates by a factor of 1.4.

Application of pulses with very high photon fluxes (e.g., $S=1$ GW/cm^2) cannot be treated within the framework of our theory since the exciton density would then be so large that exciton-exciton interaction effects would have to be taken into account, which were not considered in the present study.

Note that the numerical solution of the full set of Eq. (21) for $\xi\sqrt{|\tilde{a}(\mathbf{0},\bar{t})|^2} \gg \gamma_{ph}$, was given earlier in Ref. 22. For this case the mutual transformations between excitons and photons occur much faster than the photons escape from the crystal. This results in a substantial backward influence of the excitons on the laser pulses impinging on the crystal. The dependence of the four-wave-mixing time-integrated signal on the delay time t_d can exhibit both an oscillating (for large values of the two-photon resonance detuning) and chaotic (for small detuning values) character. However, in Ref. 22 experimentally unrealistic large laser-pulse intensities were assumed. Therefore, the results obtained there are of an academic interest only, although they can be useful for studying other physical situations. For example, when orthoexcitons are generated in Cu_2O by two photons whose frequencies strongly differ, the matrix element of the two-photon transition substantially increases,[28] and effects such as quantum beats and chaos could appear for achievable laser intensities.

VII. CONCLUSIONS

We have shown that studying the time-integrated phase-conjugated signal versus the time delay between the probe and pump pulses in a four-wave-mixing experiment facilitates studying the temporal evolution of a nonequilibrium exciton condensate over a wide range of the pulse intensities. The external field approximation yields analytical expressions which qualitatively describe the dynamics of the system and provides insight into the underlying physical pro-

cesses. The relationship for the intensity of the resulting time-integrated signal derived in this approximation is proportional to the areas of the three pulses incident on the crystal.

It is important to note that the proposed method can be used to probe the system when the exciton condensate is not generated by counter-propagating pump beams but rather arises from internal interactions of excited quasiparticles present in the system, i.e., it can be used to study the time evolution of a condensate generated by alternate means (e.g., over then gap pumping).

ACKNOWLEDGMENTS

We are grateful to S. A. Moskalenko for fruitful discussions. At Northwestern the work was supported by NSF under Grant No. 0353831.

APPENDIX: EXTERNAL FIELD APPROXIMATION FOR THE CASE OF SQUARE PULSES

We represent here the exact solutions to the system [Eq. (27)] for the case, when the probe and the pump pulses are of the square form

$$f(\bar{t}) = \zeta\left(\bar{t}, \bar{t}_0 - \frac{\bar{t}_p}{2}, \bar{t}_0 + \frac{\bar{t}_p}{2}\right), \tag{A1}$$

where

$$\zeta(\bar{t}, a, b) = H(\bar{t} - a)H(b - \bar{t})$$

and

$$H(\bar{t}) = \begin{cases} 1 & \text{at } \bar{t} \geq 0 \\ 0 & \text{at } \bar{t} < 0 \end{cases}$$

is the Heaviside step function. We then have

$$n_{ex}(\mathbf{0}, \bar{t}) = |C(t_0)|^2 |\tilde{a}(\mathbf{0}, \bar{t})|^2, \tag{A2}$$

$$\tilde{a}(\mathbf{0}, \bar{t}) = \frac{i\xi}{\gamma_{ex}}\left[\zeta\left(\bar{t}, \bar{t}_0 - \frac{\bar{t}_p}{2}, \bar{t}_0 + \frac{\bar{t}_p}{2}\right)\{e^{-\gamma_{ex}[\bar{t} - (\bar{t}_0 - \bar{t}_{p'}/2)]} - 1\} - H\left[\bar{t} - \left(\bar{t}_0 + \frac{\bar{t}_p}{2}\right)\right] 2 \sinh\left(\frac{\gamma_{ex}\bar{t}_p}{2}\right) e^{-\gamma_{ex}(\bar{t} - \bar{t}_0)}\right], \tag{A3}$$

$$n_{ph}(\mathbf{k}_4, \bar{t}) = |C(t_0)|^2 |\tilde{c}(\mathbf{k}_4, \bar{t})|^2, \tag{A4}$$

$$\tilde{c}(\mathbf{k}_4, \bar{t}) = H(\bar{t}_p - \bar{t}_d)\Phi_1(\bar{t}, \bar{t}_d) + H(\bar{t}_d - \bar{t}_p)\Phi_2(\bar{t}, \bar{t}_d), \tag{A5}$$

$$\Phi_1(\bar{t}, \bar{t}_d) = \zeta\left(\bar{t}, \bar{t}_0 + \bar{t}_d - \frac{\bar{t}_p}{2}, \bar{t}_0 + \frac{\bar{t}_p}{2}\right)\chi_1(\bar{t}, \bar{t}_d) + \zeta\left(\bar{t}, \bar{t}_0 + \frac{\bar{t}_p}{2}, \bar{t}_0 + \bar{t}_d + \frac{\bar{t}_p}{2}\right)\chi_2(\bar{t}, \bar{t}_d) + H\left(\bar{t} - \bar{t}_0 - \bar{t}_d - \frac{\bar{t}_p}{2}\right)\chi_2(\bar{t}, \bar{t}_d), \tag{A6}$$

$$\Phi_2(\bar{t}, \bar{t}_d) = \zeta\left(\bar{t}, \bar{t}_0 + \bar{t}_d - \frac{\bar{t}_p}{2}, \bar{t}_0 + \bar{t}_d + \frac{\bar{t}_p}{2}\right)\psi_1(\bar{t}, \bar{t}_d) + H\left(\bar{t} - \bar{t}_0 - \bar{t}_d - \frac{\bar{t}_p}{2}\right)\psi_1(\bar{t}, \bar{t}_d), \tag{A7}$$

$$\chi_1(\bar{t}, \bar{t}_d) = \frac{\xi^2}{\gamma_{ex} + i\delta}\left\{a_1(\bar{t}_d)\exp\left[-\gamma_{ph}\left(\bar{t} - \bar{t}_0 - \bar{t}_d + \frac{\bar{t}_p}{2}\right)\right] + a_2 \exp\left[-(\gamma_{ex} + i\delta)\left(\bar{t} - \bar{t}_0 + \frac{\bar{t}_p}{2}\right)\right] + a_3\right\}, \tag{A8}$$

$$\chi_2(\bar{t}, \bar{t}_d) = \frac{\xi^2}{\gamma_{ex} + i\delta}\left\{a_1(\bar{t}_d)\exp\left[-\gamma_{ph}\left(\bar{t} - \bar{t}_0 - \bar{t}_d + \frac{\bar{t}_p}{2}\right)\right] + b_1 \exp\left[-\gamma_{ph}\left(\bar{t} - \bar{t}_0 - \frac{\bar{t}_p}{2}\right)\right] + b_2 \exp[-(\gamma_{ex} + i\delta)(\bar{t} - \bar{t}_0)]\right\}, \tag{A9}$$

$$\chi_3(\bar{t}, \bar{t}_d) = \frac{\xi^2}{\gamma_{ex} + i\delta}\left\{a_1(\bar{t}_d)\exp\left[-\gamma_{ph}\left(\bar{t} - \bar{t}_0 - \bar{t}_d + \frac{\bar{t}_p}{2}\right)\right] + b_1 \exp\left[-\gamma_{ph}\left(\bar{t} - \bar{t}_0 - \frac{\bar{t}_p}{2}\right)\right] + c_1(\bar{t}_d)\exp\left[-\gamma_{ph}\left(\bar{t} - \bar{t}_0 - \bar{t}_d - \frac{\bar{t}_p}{2}\right)\right]\right\}, \tag{A10}$$

$$\psi_1(\bar{t}, \bar{t}_d) = \frac{-\xi^2 b_2}{\gamma_{ex} + i\delta}\left\{\exp\left[(\gamma_{ph} - \gamma_{ex} - i\delta)\left(\bar{t}_d - \frac{\bar{t}_p}{2}\right)\right]\exp[-\gamma_{ph}(\bar{t} - \bar{t}_0)] - \exp[-(\gamma_{ex} + i\delta)(\bar{t} - \bar{t}_0)]\right\}, \tag{A11}$$

$$\psi_2(\bar{t}, \bar{t}_d) = \frac{-\xi^2 b_2}{\gamma_{ex} + i\delta} 2 \sinh\left[\frac{(\gamma_{ph} - \gamma_{ex} - i\delta)t_p}{2}\right]\exp[(\gamma_{ph} - \gamma_{ex} - i\delta)t_d]\exp[-\gamma_{ph}(\bar{t} - \bar{t}_0)], \tag{A12}$$

$$a_1(\bar{t}_d) = \frac{1}{\gamma_{ex}} - \frac{\exp[-(\gamma_{ex}+i\delta)\bar{t}_d]}{\gamma_{ph}-\gamma_{ex}-i\delta}, \tag{A13}$$

$$a_2 = \frac{1}{\gamma_{ph}-\gamma_{ex}-i\delta}, \quad a_3 = -\frac{1}{\gamma_{ph}}, \tag{A14}$$

$$b_1 = \frac{\gamma_{ex}+i\delta}{\gamma_{ph}(\gamma_{ph}-\gamma_{ex}-i\delta)}, \quad b_2 = \frac{-2\sinh\left[\frac{(\gamma_{ex}+i\delta)\bar{t}_p}{2}\right]}{\gamma_{ph}-\gamma_{ex}-i\delta}, \tag{A15}$$

$$c_1(\bar{t}_d) = \frac{-2\sinh\left[\frac{(\gamma_{ex}+i\delta)\bar{t}_p}{2}\right]\exp\left[-(\gamma_{ex}+i\delta)\left(\bar{t}_d+\frac{\bar{t}_p}{2}\right)\right]}{\gamma_{ph}-\gamma_{ex}-i\delta}. \tag{A16}$$

According to formulas (A2), the dependence of the density of generated excitons versus the time $\bar{t}$ for $\bar{t} > \bar{t}_0 + \frac{\bar{t}_p}{2}$ (that is, when the pulse action has terminated) has the following form:

$$n_{ex}(\mathbf{0},\bar{t}) = \frac{4\xi^2}{\gamma_{ex}^2}|C(t_0)|^2 \sinh^2\left(\frac{\gamma_{ex}\bar{t}_p}{2}\right) e^{-2\gamma_{ex}(\bar{t}-\bar{t}_0)}. \tag{A17}$$

When the second inequality in Eq. (28) is fulfilled, we obtain

$$n_{ex}(\mathbf{0},\bar{t}) = \xi^2|C(t_0)|^2\bar{t}_p^2 e^{-2\gamma_{ex}(\bar{t}-\bar{t}_0)}. \tag{A18}$$

This formula is in accord with the result (32).

According to Eqs. (A4) and (A5), when the probe and the pump pulses are separated ($\bar{t}_d > \bar{t}_p$),

$$n_{ph}(\mathbf{k}_4,\bar{t}) = |C(t_0)|^2|\Phi_2(\bar{t},\bar{t}_d)|^2. \tag{A19}$$

Integrating Eq. (A19) over the time, we find

$$N(t_d) = \frac{\xi^4|C(t_0)|^2|b_2|^2}{\gamma_{ex}^2+\delta^2} f(\bar{t}_p,\delta)\exp[-\gamma_{ex}(\bar{t}-\bar{t}_0)], \tag{A20}$$

where

$$\begin{aligned} f(\bar{t}_p,\delta) = {} & \frac{e^{-\gamma_{ph}\bar{t}_p}}{\gamma_{ph}}[\cosh(\gamma_{ph}-\gamma_{ex})\bar{t}_p - \cos\,\delta\bar{t}_p] \\ & + \frac{\sinh\,\gamma_{ex}\bar{t}_p}{\gamma_{ex}} + \frac{\sinh\,\gamma_{ph}\bar{t}_p}{\gamma_{ph}} e^{-(\gamma_{ph}-\gamma_{ex})\bar{t}_p} \\ & + \frac{2}{(\gamma_{ph}+\gamma_{ex})^2+\delta^2}[(\gamma_{ph}+\gamma_{ex}) \\ & \times (e^{-\gamma_{ph}\bar{t}_p}\cos\,\delta\bar{t}_p - e^{\gamma_{ex}\bar{t}_p}) - \delta e^{-\gamma_{ph}\bar{t}_p}\sinh\,\delta\bar{t}_p]. \end{aligned} \tag{A21}$$

We see that the dependence of the time-integrated resulting signal N on the delay time t_d for $t_d > t_p$ is the same as the dependence of the density of the generated excitons n_{ex} versus the time t.

When the inequalities in Eqs. (28) and (29) are fulfilled, we have $f(\bar{t}_p,\delta) \approx \bar{t}_p$ and $|b_2|^2 = (\gamma_{ex}^2+\delta^2)\bar{t}_p/\gamma_{ph}^2$ and obtain the following formula:

$$N(t_d) = \frac{\xi^4|C(t_0)|^2\bar{t}_p^3}{\gamma_{ph}^2}\exp(-2\gamma_{ex}\bar{t}_d), \tag{A22}$$

that is, in accord with the result in Eq. (40).

*igor.beloussov@phys.asm.md
†j-ketterson@northwestern.edu

[1] S. A. Moskalenko and D. W. Snoke, *Bose-Einstein Condensation of Excitons and Biexcitons and Coherent Nonlinear Optics With Excitons* (Cambridge University Press, Cambridge, England, 2000).
[2] D. W. Snoke, A. J. Shields, and M. Cardona, Phys. Rev. B **45**, 11693 (1992).
[3] C. Ell, A. L. Ivanov, and H. Haug, Phys. Rev. B **57**, 9663 (1998).
[4] D. Fröhlich, G. Dasbach, G. Baldassarri Hoöger von Hoögersthal, M. Bayer, R. Klieber, D. Suter, and H. Stolz, Solid State Commun. **134**, 139 (2005).
[5] M. Inguscio, S. Stringari, and C. Wieman, *Bose-Einstein Condensation in Atomic Gases* (IOS, Amsterdam, 1999).
[6] D. Hulin, A. Mysyrowicz, and C. Benoît à la Guillaume, Phys. Rev. Lett. **45**, 1970 (1980).
[7] D. Snoke, J. P. Wolfe, and A. Mysyrowicz, Phys. Rev. Lett. **59**, 827 (1987).
[8] A. Mysyrowicz, D. W. Snoke, and J. P. Wolfe, Phys. Status Solidi B **159**, 387 (1990).
[9] D. W. Snoke, J. P. Wolfe, and A. Mysyrowicz, Phys. Rev. B **41**, 11171 (1990).
[10] J. L. Lin and J. P. Wolfe, Phys. Rev. Lett. **71**, 1222 (1993).
[11] J. I. Jang and J. P. Wolfe, Phys. Rev. B **72**, 241201(R) (2005).
[12] M. Y. Shen, S. Koyama, M. Saito, T. Goto, and N. Kuroda, Phys. Rev. B **53**, 13477 (1996).
[13] T. Goto, M. Y. Shen, S. Koyama, and T. Yokouchi, Phys. Rev. B **55**, 7609 (1997).
[14] M. Y. Shen, T. Yokouchi, S. Koyama, and T. Goto, Phys. Rev. B **56**, 13066 (1997).
[15] S. Kono, N. Naka, M. Hasuo, S. Saito, T. Suemoto, and N. Nagasawa, Solid State Commun. **97**, 455 (1996).
[16] N. Naka and N. Nagasawa, Solid State Commun. **110**, 153 (1999).
[17] Y. Sun, G. K. L. Wong, and J. B. Ketterson, Phys. Rev. B **63**, 125323 (2001).
[18] D. Fröhlich, A. Kulik, B. Uebbing, A. Mysyrowicz, V. Langer, H. Stolz, and W. von der Osten, Phys. Rev. Lett. **67**, 2343 (1991).
[19] J. I. Jang and J. B. Ketterson, Phys. Rev. B **76**, 155210 (2007).
[20] J. I. Jang, Y. Sun, S. Mani, and J. B. Ketterson, Solid State Commun. **148**, 38 (2008).
[21] J. I. Jang and J. B. Ketterson, Solid State Commun. **146**, 128

(2008).
[22] I. V. Beloussov, J. B. Ketterson, and Y. Sun, Solid State Commun. **134**, 135 (2005).
[23] H. J. Eichler, P. Gunther, and D. W. Pohl, *Laser-Induced Dynamical Grating* (Springer-Verlag, Berlin, 1980).
[24] B. Wherrett, A. Smirl, and T. Bogess, IEEE J. Quantum Electron. **19**, 680 (1983).
[25] R. J. Glauber, Phys. Lett. **21**, 650 (1966).
[26] I. V. Beloussov and V. V. Frolov, Phys. Rev. B **54**, 2523 (1996).
[27] M. Inoue and Y. Toyozawa, J. Phys. Soc. Jpn. **20**, 363 (1965).
[28] A. I. Bobrysheva, S. A. Moskalenko, and M. I. Shmigliuk, Sov. Phys. Semicond. **1**, 1469 (1967) [Fiz. Tekh. Poluprovodn. **1**, 1469 (1967) (in Russian)].